Prognostic and Therapeutic Indicator of Fluoroboronophenylalanine Positron Emission Tomography in Patients with Gliomas

Yoshinobu Takahashi, Yoshio Imahori, and Katsuyoshi Mineura

Department of Neurosurgery, Kyoto Prefectural University of Medicine, Kawaramachi Hirokoji, Kyoto, Japan

ABSTRACT

Purpose: **Boron neutron capture therapy (BNCT) for the treatment of brain tumors has attracted attention recently, and its clinical application has been progressing. We have focused on the use of BNCT with ^{10}B-boronophenylalanine, which preferentially delivers boron-10 atoms to malignant cells through the amino acid transport system. In the present study, we evaluated the long-term outcomes of treatments using ^{18}F-^{10}B-fluoroboronophenylalanine (FBPA), which is an analogue of ^{10}B-boronophenylalanine, by investigating the prognostic significance of the metabolic values and ratios of FBPA as determined by positron emission tomography (PET) in patients with gliomas.**

Experimental Design: **Our subjects were 22 patients who underwent an FBPA-PET study and were followed for at least 4 months thereafter. PET parameters, such as the rate constants K1, k2, k3, and k4, were measured before treatment. Data regarding the tumors, the contralateral normal region, and the uptake ratio of FBPA between the tumor and normal tissue 40 min after injection of the tracer were compared with survival rates after the PET treatment. The survival time and the prognostic factors were tested using a Kaplan-Meier survival curve and Cox regression analysis, respectively.**

Results: **Among the clinical parameters, the histological grade of a tumor influences survival significantly. When the survival of patients with PET parameters or ratios above the median was compared with that of patients with parameters or ratios below the median, the most significant PET parameter was the K1 value of the tumor. Median survival in patients with a tumor K1 value of 0.033 ml/min (median value) or higher was 11 months, which was significantly shorter than the 77 months in patients with a K1 value below the median ($P = 0.0006$ by generalized Wilcoxon test).**

Conclusions: **The kinetic constants of FBPA metabolism as determined by PET can be of ancillary significance in predicting the prognosis and indicating the feasibility of BNCT in patients with gliomas. The mean survival time was significantly shorter in patients with high uptakes of FBPA. A contributing factor is the K1 value, which reflects amino acid transport activity. FBPA-PET images can allow clinicians to develop treatment plans that are better tailored to the clinical features of their patients.**

INTRODUCTION

Malignant gliomas including AA[1] and GB remain fatal despite intensive combined treatment with surgery, radiotherapy, and chemotherapy. Surgical resectability depends on the size and location of the tumor, and most malignant gliomas have a propensity for infiltrative growth and dissemination. Radiotherapy and chemotherapy seem to be a more promising means of treating malignant gliomas with an infiltrative nature, even in the case of an eloquent and deep location. Although radiotherapy can be of benefit for tumor control, it may have adverse effects on the brain. Another major problem of radiotherapy for malignant gliomas is the existence of resistant tumors including a hypoxic fraction refractory to radiation. One strategy for enhancing the effectiveness of radiotherapy is to use radiosensitizers, which can attain a therapeutic dose with ordinal or lower dose yields. Boron-derivatives are essentially used in BNCT to generate the nuclear reactions (1, 2). These agents are incorporated at various degrees, and provide a high LET effect in malignant tumors showing a high boron concentration. The results of clinical trials have shown that pretreatment with boron derivatives before BNCT is feasible, although the long-term clinical results have yet to be established (3).

The introduction of PET has provided quantitative determination of physiological and metabolic processes that can be combined with anatomical information provided by anatomical imaging for an improved diagnosis. Furthermore, our understanding of the cerebral circulation and metabolism specific to tumors has also markedly improved (4–9), and an accurate assessment of these biological characteristics has improved the selection of the treatment modality specific to each tumor and the accuracy of the prognosis (10, 11). There are few reports on the *in vivo* kinetics of boron derivatives in tumors (12), and there are no reports on the prognostic implication of metabolism of boron derivatives in brain tumors. We characterized previously

Received 7/25/02; revised 7/7/03; accepted 7/17/03.

Grant support: Grants-in-Aid No. 12470296, 13470297, 13557121, 13877229, 14370443, and 15390441 for Scientific Research from the Ministry of Education, Science, Sports and Culture, Japan.

The costs of publication of this article were defrayed in part by the payment of page charges. This article must therefore be hereby marked *advertisement* in accordance with 18 U.S.C. Section 1734 solely to indicate this fact.

Requests for reprints: Yoshinobu Takahashi, Department of Neurosurgery, Kyoto Prefectural University of Medicine, Kawaramachi Hirokoji, Kamigyo-ku, Kyoto 602-8566, Japan. Phone: 81-75-251-5543; Fax: 81-75-251-5544; E-mail: yosinobu@koto.kpu-m.ac.jp.

[1] The abbreviations used are: AA, anaplastic astrocytoma; GB, glioblastoma; BNCT, boron neutron capture therapy; LET, linear energy transfer; PET, positron emission tomography; FBPA, ^{18}F-^{10}B-fluoroboronophenylalanine; BPA, ^{10}B-boronophenylalanine; DL, racemic; L, levo; AST, diffuse astrocytoma; MRI, magnetic resonance imaging; ROI, region of interest; T:N, tumor:nontumor; FDG, ^{18}F- fluorodeoxyglucose.

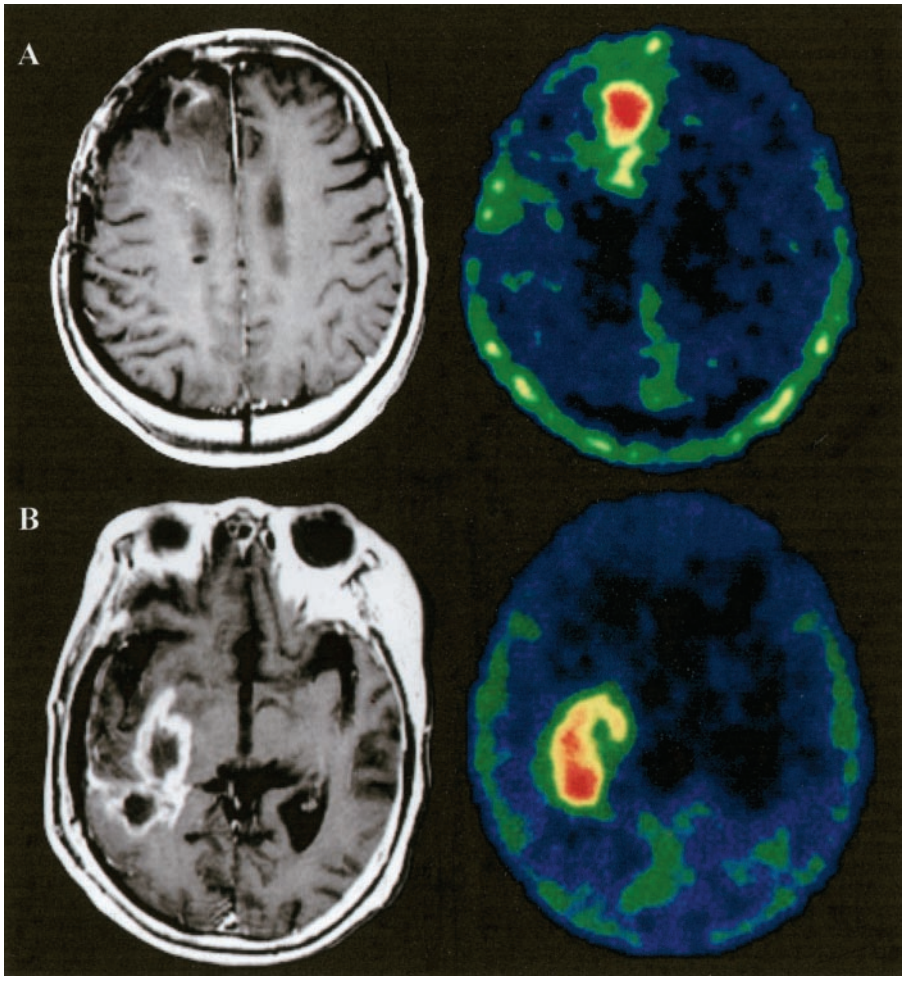

Fig. 1 *A*, MRI of case 10 (*AA*) showing a tiny enhancing tumor with a surrounding hypointense lesion in the frontal region, and FBPA accumulating intensely in the nonenhancing lesions as well as in the enhancing lesion. *Left*, enhancing T1 MRI; *right*, FBPA-PET scan. *B*, MRI and FBPA-PET of case 8 (*GB*). MRI demonstrated a heterogeneously enhancing lesion in the posterior temporal region, and FBPA uptake is exceedingly high in the lesion. *Left*, enhancing T1 MRI; *right*, FBPA-PET scan.

the kinetic constants of FBPA in gliomas (13). However, no previous studies have evaluated the correlation between the level of FBPA incorporation into tumor cells and the long-term survival rate. An FBPA-PET image can direct the use of BNCT based on clear evidence of BPA accumulation in glioma patients. The present research investigated the relationship between the long-term outcome of BNCT and the level of FBPA incorporation into glioma cells. We assessed the prognostic significance of the kinetic constants of FBPA in glioma patients and in the determination of BNCT-sensitive tumors for selective and efficient application of BNCT.

PATIENTS AND METHODS

FBPA was originally synthesized in our laboratory, as described previously (14, 15). Briefly, $^{18}F_2$ gas generated using a cyclotron was used to synthesize FBPA by using acetylhypofluorite. DL-3-(p-boronophenyl)alanine (95% ^{10}B) and L-3-(p-boronophenyl)alanine (95% ^{10}B) were purchased from Boron Biologicals, Inc. (Raleigh, NC). DL-3-(p-boronophenyl)alanine or L-3-(p-boronophenyl)alanine was dissolved in trifluoroacetic acid and acetylhypofluorite, and bubbled into a trifluoroacetic acid solution. FBPA was extracted using radio high-performance liquid chromatography with a Delta Pak, ø25 mm × 100 mm, Waters, Inc. (Milford, MA) at room temperature. FBPA solution was then filtered through a Millipore filter, MILLEX-GS 0.22 μm (Waters, Inc.) and was tested for pH, sterility, and pyrogenic properties. The final product after quality control had a specific activity of 133 GBq/mol and a radiochemical purity of >98%. Quality control of the products and the FBPA-PET study were subject to the guidelines of the PET Committee in Nishijin Hospital, Kyoto, Japan, since 1991.

The subjects were 22 patients with gliomas who underwent the FBPA-PET study. All of the patients were informed of the investigational nature of the study according to the institutional policy, and informed consent was obtained from each patient. All of the patients were treated at the Department of Neurosurgery, Kyoto Prefectural University of Medicine, Kyoto, Japan, and affiliated hospitals between July 1991 and March 2002, and they were followed-up until March 31, 2002. Representative FBPA-PET images are shown in Fig. 1. Table 1 summarizes the patient characteristics, treatment mode, and outcomes. The average age of the patients was 34 years (range, 21–78 years). All of the patients except 1 underwent tumor resection as extensively as possible before adjuvant therapy. One patient (case 19)

Table 1 Clinical summary of 22 patients examined with positron emission tomography

No.	Age	Sex	Location	Diagnosis	PS[a]	Treatment			Results (mo)[b]
						Surgery	Rad (Gy)	Chem	
1	38	M	L frontal	GB	1	R	55	Done	Died (29)
2	54	M	R frontal	GB	0	R	67 +BNCT	None	Died (16)
3	53	M	L temporoparieta	GB	1	R	50	Done	Died (13)
4	50	F	L temporoparieta	GB[c]	3	R	50	Done	Died (11)
5	67	F	R frontotemporal	GB	3	R	50	Done	Died (10)
6	51	F	R frontal	GB	1	R	50	Done	Died (10)
7	56	M	L parietooccipital	GB	0	R	— BNCT	Done	Died (7)
8	78	F	L temporal	GB	0	R	50	Done	Died (5)
9	51	F	Bil basal ganglia	GB	1	R	56	Done	Died (4)
10	39	M	R frontal	AA[c]	0	R	54	Done	Alive (131)
11	41	F	L frontal	AA[c]	0	R	50	Done	Alive (119)
12	21	F	L frontal	AA[c]	0	R	49	Done	Died (34)
13	54	F	L frontal	AA	1	R	60 +BNCT	Done	Died (16)
14	46	M	R frontal	AA[c]	0	R	60	Done	Died (16)
15	43	M	L temporal	AA	1	R	50	Done	Died (11)
16	33	M	Cellebelar	AA	2	R	50	Done	Died (4)
17	56	F	R temporoparieta	AST	2	R	50	None	Alive (129)
18	65	M	R frontal	AST	0	R	45	None	Alive (122)
19	33	F	R temporal	AST	0	—	— GK	None	Alive (77)
20	32	M	R frontal	AST	0	R	54	None	Alive (77)
21	66	M	L temporal	AST	0	R	50	None	Died (56)
22	31	M	L temporal	AST	0	R	50	Done	Died (49)

[a] PS, performance status according to Eastern Cooperative Oncology Group; R, right; L, left; Bil, bilateral; R, resection; Rad, radiation in Gy; Chem, chemotherapy; BNCT, boron neutron capturetherapy; GK, γ knife radiosurgery.
[b] Survival in months is calculated from the time of PET study.
[c] Recurrent.

received delayed surgery after radiotherapy. A neuropathologic review was performed on archival tissue in all of the cases. The histological diagnoses based on the new WHO classification were 9 GBs, 7 AAs, and 6 ASTs. One GB (case 4) and 4 AAs (cases 10–12 and 14) were studied at the time of recurrence.

All of the patients except 2 received 49–67 Gy of conventional radiation against the tumor bed using two opposing portals with a generous margin. One patient (case 19) received γ knife radiotherapy at a marginal dose of 10 Gy. Three patients (cases 2, 7, and 13) underwent BNCT. Sixteen patients were treated with combined chemotherapy including regimen A, comprised of 1-(4-Amino-2-methyl-5-pyrimidinyl)methyl-3-(2-chloroethyl)-3-nitrosourea at doses of 75–100 mg/m^2 and vincristine at doses of 1.5–2 mg/m^2, and regimen B, comprised of cisplatin at doses of 30–50 mg/m^2 and VP-16 at doses of 100–150 mg/m^2. Each chemotherapeutic agent was given i.v. at the beginning of radiation therapy and repeatedly every 6 weeks thereafter (16). The performance status was graded according to the performance status definitions of the Eastern Cooperative Oncology Group (17). Survival was calculated from the time of the PET study, which was usually within 4 weeks before the start of treatment. The follow-up time after the PET study ranged from 4 to 131 months.

The protocol for the PET measurements using a HEADTOME III (Shimadzu Co., Kyoto, Japan) has been described elsewhere (18–20). Briefly, regional FBPA incorporation into tumors and contralateral brain tissue (as a nontumor control area) was measured on dynamic PET images after an i.v. injection of FBPA at a dose of 37–55.5 MBq (1–1.5 mCi) per 10 kg of body weight. PET images were collected continuously for 60-min periods, comprising a total of 15 periods. The L-form of FBPA was given to 8 patients (cases 2, 3, 7, 13, 15, and 19–21), and the DL-form was given to 14 patients (cases 1, 4–6, 8–12, 14, 16–18, and 22). The tumor lesion on the PET images was determined using computed tomography and MRI, which were performed at levels equivalent to those for the PET scans. For quantitative measurement, oval or rectangular ROIs were placed on tumors including a peak value in various sizes from 98 to 342 mm^2 (49–171 pixels). At the corresponding level, the contralateral brain area was also chosen for ROI analysis. All of the macroscopically necrotic tumor areas were excluded when the ROIs were designated. Cases in which the active area was smaller than the above-mentioned area were excluded from the evaluation. We also confirmed that the radioactivity distribution in each pixel within the ROIs was below standard regional cerebral blood volume (18%). We designated several ROIs from tumor-affected areas and adopted the region with the highest values as a representative ROI. Regional cerebral blood volume was measured after a bolus inhalation of C^{15}O gas. The time-activity curves were corrected by the regional cerebral blood volume (21). The spatial resolution in the PET was 8.6 mm in full-width at half-maximum in plane resolution, whereas the average axial resolution was 13.6 mm.

To determine the prognostic cutoff values for the FBPA-PET parameters, the authors compared each regional value and the ratio of T:N with survival time after PET. The L-form of FBPA is a natural form that penetrates into brain tumors and normal brain tissue at a 1.85 times higher concentration than does the DL-form (13). Accordingly, we obtained the correct K1 value by multiplicity (1.85) of the DL-form K1 in patients

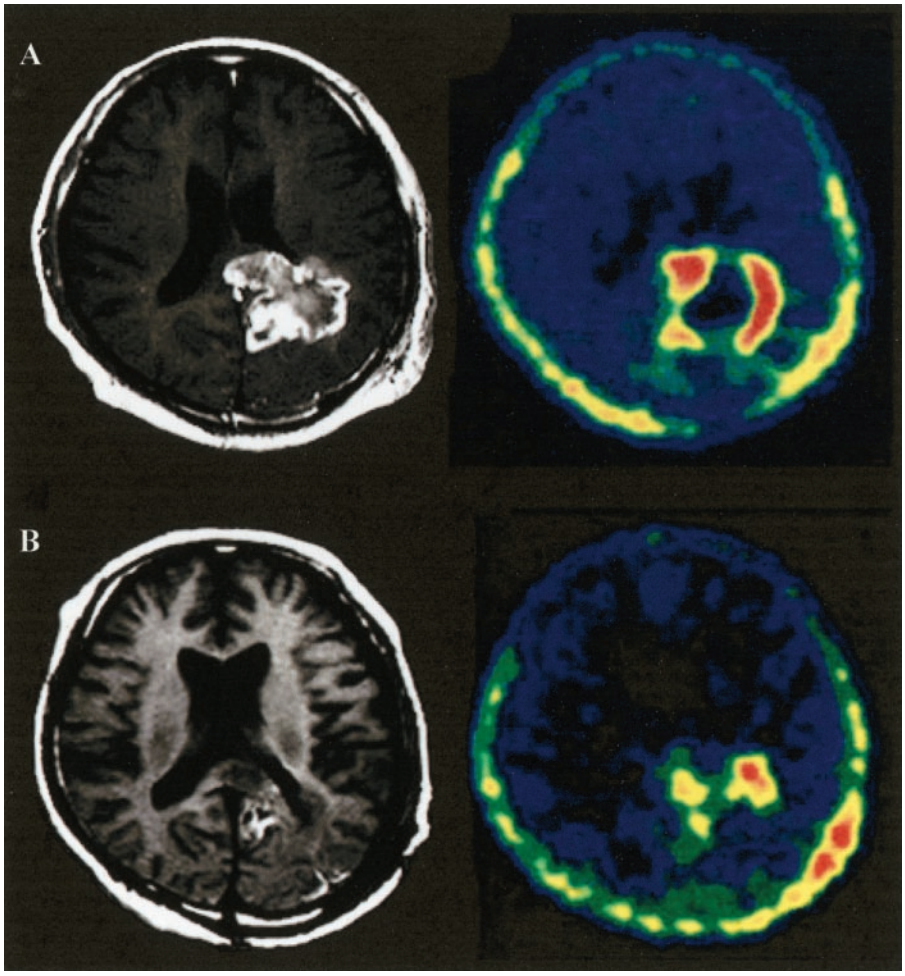

Fig. 2 Repeated MRIs and FBPA-PET scans of case 7 (*GB*) treated with BNCT. Pretherapy MRI showed an irregularly enhancing lesion around the posterior horn of the lateral ventricle, and post-therapy MRI illustrated a decrease in enhancing lesions. FBPA accumulates in the lesion in a heterogeneous fashion. After BNCT, the incorporation of FBPA was less, and the high-uptake area was more limited. BNCT was effective in prolonging both tumor-free and overall survival time. *A*, enhancing T1 MRI (*left*) and FBPA-PET (*right*) before BNCT; *B*, enhancing T1 MRI (*left*) and FBPA-PET (*right*) after BNCT.

receiving the DL-form. The study group was divided into the subgroup that had values or ratios equal to or higher than the median, and the subgroup that had values or ratios below the median. Survival between the two subgroups was also compared using the life-table method of Kaplan-Meier (22) and was statistically analyzed using the generalized Wilcoxon test (23). Monovariate and multivariate analysis were performed using the Cox, nonparametric proportional hazards regression model (24), and using StatView 5.0 (SAS Institute Inc., Cary, NC) to identify important prognostic factors relating to survival. *P*s < 0.05 were considered statistically significant.

For the BNCT, we prepared an L-BPA fructose-complex solution, according to the method described by Yoshino *et al.* (25). This complex dissociates and reaches equilibrium between free molecules and the complex in the diluted condition present in plasma. The molar concentration of the L-BPA-fructose complex was 115 mM and the ^{10}B-concentration was 5.52 mM. The molar ratio of L-BPA to fructose was 1:2.57. For the clinical use of BNCT, the amount of L-BPA-fructose solution used was 600–800 ml, and the infusion requires about 60–80 min. In the convolution method (26, 27), estimated values of tissue ^{10}B-concentration of L-BPA can be calculated by the rate constants (K1, k2, k3, and k4) for L-FBPA obtained by PET for each patient. The input function of L-BPA can be determined by blood sampling over 1–2 h. The tumor ^{10}B-level can be calculated by convoluting the input function of Cp(t) to a weight function using K1, k2, k3, and k4 (13, 27).

For treatment, a craniotomy was performed in the nuclear reactor (The Research Reactor Institute, Kyoto University, Kyoto, Japan), and L-BPA-fructose complex was then drip-infused. Neutron irradiation was then performed. Case 7 was a 56-year-old male with GB treated using a PET-BNCT system (Fig. 2). The T:N ratio in this case ranged from 1.43 to 2.78 in five intratumoral ROIs. Such intratumoral variability is mainly due to both biological and histological heterogeneity. The highest area was chosen as a representative ratio, because the most active portion regulates the prognosis. Before neutron irradiation, PET was performed using L-FBPA, and showed a high incorporation of boron with a T:N ratio of 2.78 and a ^{10}B concentration estimated to be 36 ppm in the tumor. The BNCT procedures proceeded as follows: (*a*) collimation of the tumor (7.5×7.5 cm) by craniotomy; (*b*) placement of a gold wire intracranially through a drainage tube; (*c*) alveolar polyethylene balls with a diameter of 1 cm packed into the dead space; (*d*) after infusion of 180 mg/kg of L-BPA (containing 8.6 mg/kg of ^{10}B) over 60 min, thermal neutron irradiation initiated; and (*e*)

surface maximum value of thermal neutron fluence at 1.5×10^{13} n/cm^2 for 2 h. The tumor received a physical dosage of 11 Gy.

RESULTS

Survival Time. Table 1 includes the results and survival times for all of the patients. At the final follow-up date, March 31, 2002, 6 patients (cases 10, 11, and 17–20) had survived for at least 77 months (range, 77–131 months). The other patients had died by this date, and the survival time varied between 4 and 56 months, with a median of 12 months. Among the clinical parameters, the histological grade was the most important factor in the prognosis of gliomas. At the final follow-up, 4 of 6 patients with AST were still alive, whereas all but 2 of the patients with GB or AA died within 34 months. In the limited cohort of 16 patients with malignant gliomas, those with AA (16 months) and GB (10 months) showed only a slight difference in median survival time (Fig. 3).

Kinetic Measurement. Table 2 shows the kinetic measurements determined by PET. A highly significant difference in K1, β, and γ was observed between the tumor and the corresponding normal region ($P < 0.001$, Student's t test). Patients demonstrating K1 measurements at the median (0.033) or higher had a median survival time of 11 months, whereas patients with a value below the median had a significantly longer median survival time of 77 months ($P = 0.0006$; Fig. 4).

PET Parameters and Survival. To determine whether PET parameters were significant indicators of biological tumor activity in gliomas, we compared survival time between patients with values or ratios equal to or higher than the median, and patients with values or ratios below the median (Table 3). There was a significant relationship between survival and tumor K1, k3, and γ ($P < 0.05$ by generalized Wilcoxon test). Median survival for patients with high-K1 tumors was 11 months compared with a median survival of 77 months for those with low-K1 tumors (Fig. 4). None of the PET parameters obtained in normal brain areas correlated with survival. However, the ratio of K1 and γ between the tumor and normal tissue was a significant predictor of patient survival. Clinical and PET parameters were tested as independent prognostic variables using a Cox regression analysis. Table 4 summarizes the significant variables. Monovariate analysis indicated that among the clinical parameters, the histological grade was the most critical factor predicting survival. Performance status was an insignificant factor in this study. Patient characteristics such as age and sex were not significant. Survival did not correlate with the mode of chemotherapy. Again, tumor K1, k3, γ, and T:N ratio correlated well with survival. In the multivariate analysis with stepwise variable selection, we eliminated the corresponding variables from rate constants. Tumor K1 was the most significant prognostic variable ($P = 0.0002$).

Table 2 PET parameters in 22 patients with astrocytic tumors

PET parameters	Tumor	Non-tumor	T:N ratio
K1 (min^{-1})			
Mean	0.037[b]	0.010	3.600
SD	0.022	0.003	1.887
Median	0.033	0.011	3.667
k2 (min^{-1})			
Mean	0.032	0.023	1.700
SD	0.016	0.013	1.107
Median	0.034	0.025	1.378
k3 (min^{-1})			
Mean	0.023	0.030	1.223
SD	0.008	0.017	1.712
Median	0.025	0.031	0.813
β (Dv)[a]			
Mean	0.349[b]	0.073	6.068
SD	0.229	0.040	5.363
Median	0.286	0.062	4.756
γ (min^{-1})			
Mean	0.016[b]	0.006	2.555
SD	0.008	0.002	0.917
Median	0.015	0.006	2.637

[a] β, tracer; γ, degree of the accumulation rate.
[b] Significant at the levels of $P = 0.001$ from the corresponding values of normal.

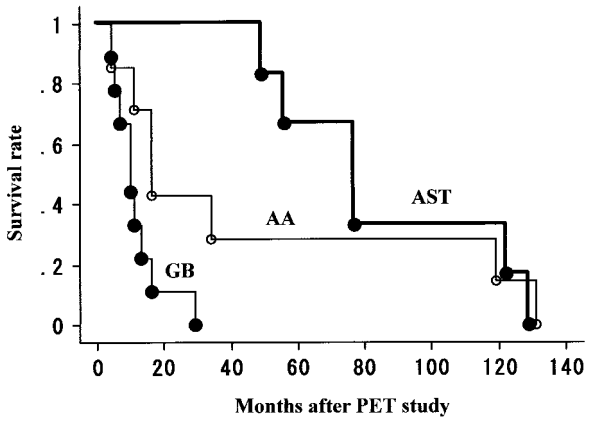

Fig. 3 Kaplan-Meier survival curves of gliomas according to histology. Survival shows a significant difference by histology ($P = 0.02$ by the generalized Wilcoxon test). Median survival times were 77, 16, and 10 months for AST, AA, and GB, respectively.

DISCUSSION

Prognostic Implication. PET offers quantitative measurements and information on blood flow and metabolism using a variety of positron tracers. Various prognostic factors such as patient age, performance status, and histology have been proposed in cerebral gliomas (28–31). Among these prognostic variables, the histological grade is considered highly predictive. Histology, especially when judged from biopsied specimens, may easily underestimate the degree of tumor malignancy. The most reliable approach is to use a large amount of tumor tissue containing the most malignant parts of a tumor. Among high-grade gliomas, the histological grade showed less predictive value, due, most likely, to the fact that the specimens did not contain the most aggressive part of the tumor, because malignant gliomas consist of heterogeneous tissue components including viable portions, central necrosis areas, and peritumoral infiltration areas. Furthermore, there is a critical disadvantage in obtaining a large-volume tissue sample during brain tumor surgery, because the resected amounts of tumor tissue are often limited, particularly when tumors are adjacent to or in eloquent

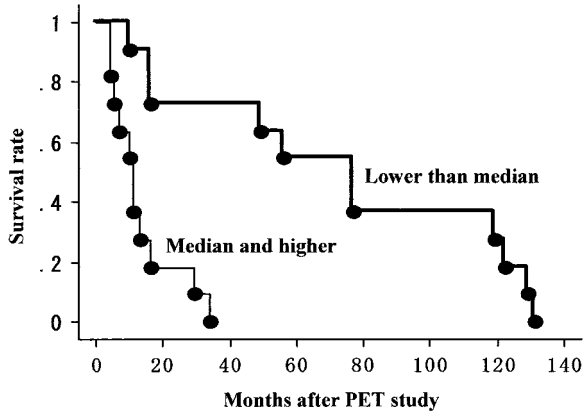

Fig. 4 Kaplan-Meier survival curves for 11 patients with tumor K1 lower than the median (0.033) and 11 patients with the ratio equal to or higher than the median. There was a significant difference in survival ($P = 0.0006$) on generalized Wilcoxon test.

Table 3 PET parameters and median survival time

PET parameters	Median survival time (mo)[a]		
	Tumor	Nontumor	T:N ratio
K1			
Low (n = 11)	77	16	77
High (n = 11)	11	16	11
P	0.0006	ns	0.0067
k2			
Low (n = 11)	49	16	34
High (n = 11)	11	16	16
P	ns	ns	ns
k3			
Low (n = 11)	77	29	16
High (n = 11)	11	11	16
P	0.0079	ns	ns
β			
Low (n = 11)	49	16	56
High (n = 11)	13	16	11
P	ns	ns	ns
γ			
Low (n = 11)	77	16	77
High (n = 11)	10	16	11
P	<0.0001	ns	0.0009

[a] mo, month; Low, patients with values lower than the median; High, patients with values equal to or higher than the median; ns, not significant.

areas. Because PET can image the entire tumor, it, therefore, overcomes such problems with histological evaluation alone. PET parameters were useful indicators predicting patient survival in cases of glioma. Our monovariate analysis indicated that K1, k3, γ, and T:N ratio were significant prognostic factors, along with the histological grade. The multivariate analysis based on the regression model using PET covariates showed that the tumor K1 was the most significant factor predicting survival. The clinical parameters such as the performance status were not significant, because the model already included these parameters. The K1 was strongly correlated with the histological grade. It is an important finding that K1 values, which can be obtained during a noninvasive PET examination, can predict the histological grade of malignancy in gliomas.

Selection of BNCT-Targeted Tumor. Radiotherapy is potentially beneficial in tumor control; however, its effectiveness appears to be modest in the treatment of gliomas. One reason for this may be the limited doses, at most 60 Gy, that is usually administrated to the brain and its lesions. To increase the therapeutic efficacy of radiation, we have sought to increase the dose effectiveness by providing high-LET effects. BNCT is a high-LET radiotherapy in systemic malignancies including brain tumors and melanoma using BPA (32). Because BPA is incorporated into tumor cells in the brain parenchyma, attention is currently being focused on the therapeutic value of BNCT using BPA, because ^{10}B-mercaptoundecahydrododecaborate is not specifically incorporated into tumor cells. In addition, it is difficult to investigate the level of incorporation of BPA itself, a neutron capture compound, into glioma cells and its association with malignancy. In our study, kinetic parameters (rate constants) obtained by FBPA-PET could be used to determine the ^{10}B-concentration in a brain tumor (26, 27). We found that these parameters were generally the same for each grade, and can readily be used by therapists for pretreatment assessment. FBPA is accepted as an indicator of the amino acid transport process through blood brain barrier and in the tumor cells. The FBPA-PET method was useful for measuring FBPA incorporation in gliomas and even for evaluating the histological diagnosis, because the small amounts of tissue available from a biopsy was insufficient.

The therapeutic results are still disappointing in gliomas, despite continuous efforts, and recent progress in their diagnosis and the treatment. A major problem remains the random application of treatment modes for gliomas, whether they are sensitive or resistant. BNCT trails have shown no satisfactory results (33). One of the reasons for the poor results is the concentration of BPFA at the time of neutron capture therapy. We were able to find no information on the *in vivo* concentration of boron derivatives during the time of BNCT. To date, a number of attempts have been made to determine the concentration mainly on tissue obtained from resection. These failures represent a critical disadvantage in the application of efficient therapy based on biological properties of gliomas, because prior surgery is necessary and because the amount of resected tissue is often

Table 4 Regression model of survival analysis

Covariate	Monovariate analysis		Multivariate analysis	
	χ^2	*P*	χ^2	*P*
Clinical parameters				
Age	1.326	0.250		
Gender	0.233	0.630		
Histologic grade	10.063	0.007		
Performance status	6.869	0.076		
Chemotherapy	2.832	0.092		
PET parameters				
K1	7.961	0.005	13.595	0.0002
k2	0.986	0.321	3.770	0.0522
k3	0.831	0.362	8.344	0.0039
β	9.069	0.219		
γ	9.796	0.002		

limited, particularly during an exploration biopsy. One strategy, which aims to enhance the therapeutic results of BNCT, is the selective application of treatment to gliomas that are sensitive to BNCT. In the present study, we attempted to find *in vivo* evidence of boron derivatives in gliomas before treatment and to establish an imaging method using PET that was applicable to BNCT.

FBPA Uptake and Activity of the Amino Acid Transport. In our previous study, kinetic analysis using PET demonstrated that the uptake of the L-form of FBPA is better than that of the DL-form. This result is due to the active transport via L-forms of large neutral amino acids transporter. Because it is solely the difference in the form of stereo-anomers that determines K1, the amount of uptake is strongly dependent on K1. The DL-form is distinguished from the L-form by amino acid transport, and consequently K1 provided by the L-form is a quantitative parameter of the amino acid transport process. Therefore, it is likely that amino acid transport, which is a biologically significant process, is represented as K1 provided by the L-form of FBPA. Because k2 is not affected by the stereo-anomers, the partition rate (K1/k2) is also dependent only on K1. In cases of GB, for example, the average K1 for the L-form was 1.6–1.9 times that for the DL-form. An approximately similar magnitude of difference in the average K1 was also noted in cases of AA, AST, and in the contralateral cortex, and consequently the K1 provided by the DL-form was corrected in the total cases of gliomas in multiples of 1.85. The absence of an evident difference in k3 between the DL- and L-forms suggests that k3 represents phenomena that are not dependent on the L-form. This process may not be due to any specific enzymatic reaction. Although direct studies are needed on this issue, we speculate that ^{18}F activity is pooled within cells due to polarization of FBPA by a nonenzymatic reaction rather than due to metabolism via the amino acid anabolic pathway (25).

Rate Constant K1 and Tumor Malignancy. The K1 value differed significantly between the malignant group (GB and AA) and the benign group (AST). These results indicate that the FBPA uptake capacity, associated with tumor grade, is dependent on K1, which is an indicator of the amino acid transport process. The average of γ, which is an indicator of uptake capacity, was somewhat high in AA cases, probably because AA tumors are necrosis-free, unlike GB. In terms of these parameters, there was no marked difference between GB and AA. These tendencies were seen irrespective of the use of the DL- or L-form. It is well known that large neutral amino acids including FBPA pass through blood brain barrier via transporters located in brain capillary endothelial cells (34–37). Considering the influence of blood flow, a mean K1 of 0.1 ml/100 g/min suggests that the tracer transfer mechanism depends on the transporter capacity, but not on tumor blood flow, based on the Renkin-Crone model (38). Therefore, we excluded the amino acid uptake mechanism by diffusion with increased blood flow in tumor blood vessels. The properties of FBPA are similar to those of FDG in transport mechanisms. However, FBPA is not metabolized in cells, unlike FDG. The accumulation of FBPA, which was evaluated in the present study, may depend only on active uptake by the transporter. Therefore, K1 is the most important factor in this study. On the basis of the above discussion, only K1 was significantly correlated with the prognosis of a glioma, which does not contradict the above properties.

Two factors are considered for an increase in K1, which is a factor contributing to amino acid uptake by tumors. In the Renkin-Crone model, K1 is determined by permeability and surface area. Considering the mean T:N ratio 3.6 of K1 in GB, it is interesting to know whether the permeability or the surface area changed. If the cell density was similar, the number of transporters per cell did not increase, and an increase in the number of cells may have been reflected.

The accumulation mechanism of FBPA depends on amino acid transport systems. K1 represents the permeability of amino acid transport systems. In the present study, the tumor K1 showed a high value in contrast to a low value in the normal brain, indicating a markedly high accumulation of FBPA in gliomas relative to the normal brain. In contrast, FDG undergoes phosphorylation within cells, and k3 is an important factor for FDG incorporation. FDG accumulates in gliomas as well as in normal brain tissue. Therefore, FBPA provides a better delineation and identification of tumors, and easily visualizes gliomas as hot lesions.

PET with a variety of tracers and a multidisciplinary approach can provide qualitative and quantitative data for the diagnosis and prognosis of gliomas. The tracers should be selected so that they provide crucial information required in the diagnosis and therapy application for gliomas. Additional PET studies using a variety of tracers, and particularly with FDG, are clearly warranted. FBPA-PET is a practical and clinically useful method for making a prognosis and for determining whether tumors will be sensitive or resistant to BNCT in gliomas.

ACKNOWLEDGMENTS

We thank the staff of the Cyclotron Unit, Nishijin Hospital (Kyoto, Japan) for their cooperation and the members of the Department of Neurosurgery, Kyoto Prefectural University of Medicine (Kyoto, Japan) for providing clinical information.

REFERENCES

1. Barth, R. F., Soloway, A. H., and Fairchild, R. G. Boron neutron capture therapy of cancer. Cancer Res., *50:* 1061–1070, 1990.

2. Coderre, J. A., and Morris, G. M. Review: The radiation biology of boron neutron capture therapy. Radiat. Res., *151:* 1–18, 1999.

3. Diaz, A. Z., Coderre, J. A., Chanana, A. D., and Ma, R. Boron neutron capture therapy for malignant gliomas. Ann. Med., *32:* 81–85, 2000.

4. DiChiro, G., DeLaPaz, R. L., Brooks, R. A., Sokoloff, L., Kornblith, P. L., and Smith, B. H. Glucose utilization of cerebral gliomas measured by [^{18}F]fluorodeoxyglucose and positron emission tomography. Neurology, *32:* 1323–1329, 1982.

5. Hubner, K. F., Purvis, J. T., Mahaley, S. M., Robertson, J. T., Rogers, S., and Gibbs, W. D. Brain tumor imaging bypositron emission computed tomography using ^{11}C-labeled amino acids. J. Comput. Assist. Tomogr., *6:* 544–550, 1982.

6. DiChiro, G. Positron emission tomography using [^{18}F]fluorodeoxyglucose in brain tumors: a power diagnostic and prognostic tool. Investig. Radiol., *22:* 360–371, 1986.

7. Derlon, J. M. Bourdet, C., Bustany, P., Chatel, M., Therson, J., Darcel, F. [^{11}C]L-methionine uptake in gliomas. Neurosurgery, *25:* 720–728, 1989.

8. Coleman, R. E., Hoffman, J. M., Hanson, M. W., Sostman, H. D., and Schold, S. C. Clinical application of PET for the evaluation of brain tumors. J. Nucl. Med., *32:* 616–622, 1991.

9. Strauss, L. G., and Conti, P. S. The applications of PET in clinical oncology. J. Nucl. Med., *32:* 623–648, 1991.

10. Hanson, M. W., Glantz, M. J., Hoffman, J. M., Friedman, A. H., Burger, P. C., and Schold, S. C. FDG-PET in the selection of brain lesions for biopsy. J. Comput. Assist Tomogr., *15:* 796–801, 1991.

11. Levivier, M., Goldman, S., Bidaut, L. M., Luxen, A., Stanus, E., and Przedborski, S. Positron emission tomography-guided stereotactic biopsy. Neurosurgery, *31:* 792–797, 1992.

12. Kabalka, G. W., Smith, G. T., Dyke, J. P., Reid, W. S., Longford, C. P. D., Roberts, T. G., Reddy, N. K., and Hubner, K. F. Evaluation of fluorine-18-BPA-fructose for boron neutron capture treatment planning and hemodynamic evaluation of gliomas using positron emission tomography. J. Nucl. Med., *38:* 1762–1767, 1997.

13. Imahori, Y., Ueda, S., Ohmori, Y., Kusuki, T., Ono, K., Fujii, R., and Ido, T. Fluorine-18-labeled fluoroboronophenylalanine and PET in patients with glioma. J. Nucl. Med., *39:* 325–333, 1998.

14. Ishiwata, K., Ido, T., and Mejia, A. A. Synthesis and radiation disimetry of 4-borono-2-[^{18}F]fluoro-D, L-phenylalanine: a target compound for PET and boron neutron capture therapy. Appl. Radiat. Isot., *42:* 325–328, 1991.

15. Mishima, Y., Imahori, Y., Honda, C., Hiratsuka, J., Ueda, S., and Ido, T. *In vivo* diagnosis of human malignant melanoma with positron emission tomography using specific melanoma-seeking ^{18}F-DOPA analogue. J. Neurooncol., *33:* 163–169, 1997.

16. Mineura, K., Watanabe, K., and Kowada, M. Supratentorial malignant gliomas treated with split course radiotherapy plus chemotherapy of ACNU and FT. Int. J. Oncol., *2:* 457–461, 1993.

17. Oken, M. M., Creech, R. H., Tormey, D. C., Horton, J., Davis, T. E., and McFadden, E. T. Toxity and response criteria of the Eastern Cooperative Oncology Group. Am. J. Clin. Oncol., *5:* 649–655, 1982.

18. Frackowiak, R. S. J., Lenzi, G. L., Jones, T., and Heather, J. D. Quantitative measurement of regional cerebral blood flow and oxygen metabolism in man using ^{15}O and positron emission tomography: theory, procedure, and normal values. J. Comput. Assist. Tomogr., *4:* 727–736, 1980.

19. Kanno, I., Miura, S., Yamamoto, S., Iida, H., Murakami, M., and Takahashi, K. Design and evaluation of a positron emission tomography: Headtome III. J. Comput. Assist. Tomogr., *9:* 931–939, 1985.

20. Sasaki, H., Kanno, I., Murakami, M., Shishido, F., and Uemura, K. Tomographic mapping of kinetic rate constants in the fluorodeoxyglucose model using dynamic positron emission tomography. J. Cereb. Blood Flow. Metab., *6:* 447–454, 1986.

21. Phelps, M. E., Huang, S. C., Hoffman, E. J., and Kuhl, D. E. Validation of tomographic measurement of cerebral blood volume with C-11 labeled carboxyhemoglobin. J. Nucl. Med., *20:* 328–334, 1979.

22. Kaplan, E. L., and Meier, P. Non parametric estimation for incomplete observations. J. Am. Stat. Assoc., *52:* 457–481, 1958.

23. Gehan, E. A generalized Wilcoxon test for comparing arbitrarily singly-censored samples. Biometrika., *52:* 203–224, 1956.

24. Cox, D. Regression models and life tables. J. R. Stat. Soc (B)., *34:* 187–202, 1972.

25. Yoshino, K., Mori, Y., and Kakihana, H. Chemical modeling with p-boronophenylalanine for boron accumulation to and release from melanoma. *In:* Y. Mishima, ed. Cancer Neutron Capture Therapy, pp. 81–90. New York: Plenum Press, 1996.

26. Imahori, Y., Ueda, S., Ohmori, Y., Sakae, K., Kusuki, T., Kobayashi, T., Takagaki, M., Ono, K., Ido, T., and Fujii, R. Positron emission tomography-based boron neutron capture therapy using boronophenylalanine for high-grade gliomas. Part I. Clin. Cancer Res., *4:* 1825–1832, 1998.

27. Imahori, Y., Ueda, S., Ohmori, Y., Sakae, K., Kusuki, T., Kobayashi, T., Takagaki, M., Ono, K., Ido, T., and Fujii, R. Positron emission tomography-based boron neutron capture therapy using boronophenylalanine for high-grade gliomas. PartII. Clin. Cancer Res., *4:* 1833–1841, 1998.

28. Green, S. B., Byar, D. P., Walker, M. D., Pistenmaa, D. A., Alexander, E., and Batzdorf, U. Comparisons of camustine, procarbazine and high-dose methylprednisolone as additions to surgery and radiotherapy for the treatment of malignant gliomas. Cancer Treat. Rep., *67:* 121–132, 1983.

29. Nelson, J. S., Tsukada, Y., Schoenfeld, D., Fulling, K., Lamarche, J., and Peress, N. Necrosis as a prognostic criterion in malignant supratentorial, astrocytic gliomas. Cancer (Phila.), *52:* 550–554, 1983.

30. Murovic, J., Krzystof, T., Wilson, C. B., Hoshino, T., and Levin, V. Computerized tomography in the prognosis of malignant cerebral gliomas. J. Neurosurg., *65:* 799–806, 1986.

31. A Report of the Medical Research Council Brain Tumour Working Party. Prognostic factors for high-grade malignant gliomas: development of a prognostic index. J. Neurooncol., *9:* 47–55, 1990.

32. Mishima, Y., Honda, C., Ichihashi, M., Obara, H., Hiratsuka, J., Fukuda, H., Karashima, H., Kobayashi, T., Kanda, K., and Yoshino, K. Treatment of malignant melanoma by single thermal neutron capture therapy with melanoma-seeking ^{10}B-compound. Lancet, *12:* 388–389, 1989.

33. Chanana, A. D., Capala, J., Chadha, M., Coderre, J. A., Diaz, A. Z., Elowitz, E. H., Iwai, J., Joel, D. D., Liu, H., Ma, R., Pendzick, N., Peress, N. S., Shandy, M. S., Slatkin, D. N., Tyson, G. W., and Wielopolski, L. Boron neutron capture therapy for glioblastoma multiforme: interim results from the phase I/II dose-escalation studies. Neurosurgery, *44:* 1182–1192, 1999.

34. Padridge, W. M. Kinetics of competitive inhibition of neutral amino acid transport across the blood-brain barrier. J. Neurochem., *28:* 103–108, 1977.

35. Padridge, W. M. Brain metabolism. A perspective from the blood-brain barrier. Physiol. Rev., *63:* 1481–1535, 1983.

36. Smith, Q. R. The blood-brain barrier and the regulation of amino acid uptake and availability to brain. Adv. Exp. Med. Biol., *291:* 55–71, 1991.

37. Smith, Q. R., Momma, S., Aoyagi, M., and Rapoport, S. I. Kinetics of neutral amino acid transport across the blood-brain barrier. J. Neurochem., *49:* 1651–1658, 1987.

38. Crone, C. The permeability of capillaries in various organs as determined by use of the "indicator diffusion" method. Acta Physiol. Scand., *58:* 292–305, 1963.